

Accepted Manuscript

Structure of Cationic Surfactant Micelles from Molecular Simulations of Self-Assembly

Miguel Jorge

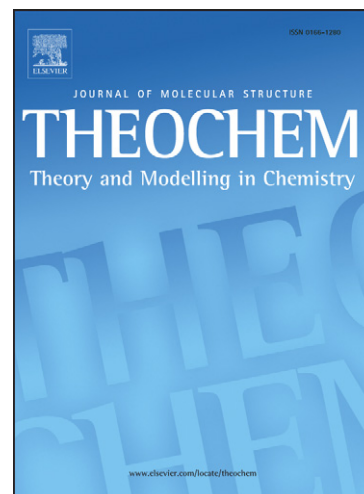
PII: S0166-1280(09)00673-3
DOI: [10.1016/j.theochem.2009.09.054](https://doi.org/10.1016/j.theochem.2009.09.054)
Reference: THEOCH 11856

To appear in: *Journal of Molecular Structure: THEOCHEM*

Received Date: 3 August 2009
Revised Date: 25 September 2009
Accepted Date: 30 September 2009

Please cite this article as: M. Jorge, Structure of Cationic Surfactant Micelles from Molecular Simulations of Self-Assembly, *Journal of Molecular Structure: THEOCHEM* (2009), doi: [10.1016/j.theochem.2009.09.054](https://doi.org/10.1016/j.theochem.2009.09.054)

This is a PDF file of an unedited manuscript that has been accepted for publication. As a service to our customers we are providing this early version of the manuscript. The manuscript will undergo copyediting, typesetting, and review of the resulting proof before it is published in its final form. Please note that during the production process errors may be discovered which could affect the content, and all legal disclaimers that apply to the journal pertain.



Structure of Cationic Surfactant Micelles from Molecular Simulations of Self-Assembly

Miguel Jorge

Laboratory of Separation and Reaction Engineering, Associate Laboratory LSRE/LCM,
Faculdade de Engenharia, Universidade do Porto, Rua Dr. Roberto Frias, 4200-465 Porto,
Portugal

Email address: miguel.jorge@fc.up.pt

Abstract

Molecular dynamics simulations of self-assembly of n-decyltrimethylammonium bromide surfactants were performed using an atomistic model, and a detailed analysis of the spontaneously formed micellar aggregates was carried out. This allowed for a detailed study of the structure of cationic surfactant micelles free from any *a priori* assumptions regarding their size and shape. Atomic radial distribution functions, radial density profiles and bivariate water orientation distributions were computed. Together, they show the presence of a dry micelle core, with a hydrophobic environment similar to a liquid alkane, a well-defined head-group layer at the interface, and an outer layer of strongly bound bromide counterions. Water molecules penetrate the micelle as far as the innermost head site, adopting a sequence of orientations that is akin to that observed at planar interfaces with vapor or immiscible organic solvents. Water molecules at

the exterior of the micelle are highly polarized by the electrical double-layer formed by cationic head-groups and bromide anions, orienting themselves with their dipole vector pointing towards the micelle core.

Key words: molecular simulation; amphiphilic; thermodynamics; mesostructure; interfaces.

1. Introduction

Surfactant molecules are typically composed of a hydrophilic “head” and a hydrophobic “tail”. This amphiphilic structure gives rise to the formation of extremely rich phase diagrams in aqueous solutions, which depend on factors such as the type of surfactant (anionic, cationic or neutral), its concentration, the temperature, and the presence of co-solvent or dissolved electrolytes [1]. Due to these fascinating properties, surfactants are important in several biological, chemical and physical processes, have widespread practical applications, and have been the subject of numerous experimental [2] and theoretical [3] studies. A particular aspect that is rather difficult to probe experimentally is the detailed structure of surfactant aggregates (e.g., micelles) at the molecular level. Thus, molecular simulation techniques have been widely applied to characterize micellar solutions (see the review by Shelley and Shelley [3] and references therein). In this paper, molecular dynamics (MD) simulations are applied to study the structural properties of n-decyltrimethylammonium bromide (DeTAB) micelles in water. This work was performed in the context of a project devoted to studying the formation mechanism of periodic mesoporous silica materials by molecular simulation [4-6], and the choice of surfactant was motivated by its use as a template for the synthesis of those materials. Furthermore, DeTAB belongs to the widely studied family of quaternary ammonium salts, commonly considered as representative examples of cationic surfactants.

Most previous simulation studies at the atomistic level have been carried out on systems composed of single pre-formed micelles solvated in water [3], but only a few have focused on the structure of micelles composed of quaternary ammonium surfactants. Böcker et al [7] generated a spherical n-decyltrimethylammonium chloride micelle composed of 30 surfactants surrounded by 2166 water molecules. They observed that during their 275 ps simulation runs, the shape of the micelle changed from spherical to slightly prolate ellipsoid. Their radial density profiles and probability distributions were rather noisy, but nevertheless showed that the interior of the micelle was completely dry, with water penetrating only as far as the well-defined layer of head-group atoms. The chloride counterions were seen to associate with the cationic head groups, forming a diffuse layer on the outside of the micelle. Similar conclusions were drawn by Piotrovskaya et al. [8], who analyzed both pre-formed spherical and cylindrical cetyltrimethylammonium chloride micelles. They went on to study the effect of several additives on the micelle structure, obtaining results that were in qualitative agreement with experiments. The most detailed study to date was performed recently by Pal et al. [9] on a spherical micelle formed by 47 DeTAB molecules surrounded by 5834 water molecules. They confirmed that water molecules penetrated only as far as the first tail atom, and observed that they were preferentially found in the regions between two methyl head groups. By carrying out a detailed study of hydrogen bond dynamics, they were able to show that such “buried” water molecules display a significantly slower dynamic response than bulk water.

The studies mentioned above have yielded valuable information but have the disadvantage of relying on *a priori* assumptions regarding the structure and size of the aggregate. A much more attractive alternative would be to study the properties of micelles resulting from a direct simulation of the self-assembly process. However, such simulations are much more computationally intensive, and have for many years been restricted to very small system sizes and/or short runs [10-13]. As a consequence, micellar properties obtained in those systems

typically suffer from large statistical uncertainties [11]. Recently, the large increase in computer power based on massively parallel machines has made possible the direct simulation of surfactant self-assembly using atomistic models for relatively large systems, in which several micelles were formed [14]. The present paper follows from that study and concentrates on the detailed properties of DeTAB micelles generated from large self-assembly simulations, taking advantage of recent developments in the molecular-level description of liquid/liquid interfaces [15-18]. A particular aspect that is emphasized in this paper is the orientation of water molecules at the surface of the micelle, determined using the concept of a bivariate angle distribution. This method has shed new light onto the structure of water at planar interfaces with vapor [18] or immiscible organic solvents [15-17], and is applied here for the first time to curved water/micelle interfaces. In the next section, the computational methods are briefly described, followed by a presentation and discussion of the results. The main conclusions of the paper are summarized in section 4.

2. Computational Methods

MD simulations were performed using version 3.3 of the GROMACS simulation package [19,20]. The Verlet leapfrog algorithm [21] with a time step of 2 fs was used to integrate the equations of motion. All simulations were carried out in the NpT ensemble, with the temperature fixed at 298.15 K by applying the Nosé-Hoover thermostat [22,23], and the pressure fixed at 1 bar by applying the Parrinello-Rahman barostat [24]. The potential energy of the system was computed as the sum of harmonic angle bending terms, torsional Ryckaert-Bellemans terms, Lennard-Jones repulsion/dispersion terms, and Coulomb electrostatic terms. All bond lengths were held rigid by applying the LINCS constraint algorithm [25]. A twin-range cutoff scheme (inner radius of 1.0 nm and outer radius of 1.2 nm) was applied to the Lennard-Jones interactions, together with a long-range dispersion correction for both energy and pressure. Long-range

electrostatic interactions were handled using the particle-mesh Ewald method [26] with a real-space cutoff of 1.0 nm. The rigid SPC/E potential model [27] was chosen to represent the water molecules, while the n-decyltrimethylammonium cations (DeTA⁺) were represented by a united atom model, in which each CH₃ and CH₂ group is described by a single effective interaction center. Parameters for the head group were taken from Jorgensen and Gao [28], while those for the aliphatic tail were obtained from Smit et al. [29]. The performance of this model in describing surfactant aggregates has been shown to be equivalent to a more realistic but more computationally demanding all-atom model [14]. A schematic diagram of the DeTA⁺ cation, with the nomenclature adopted for each site, is shown in Figure 1. The reader is referred to a previous publication [14] for further details concerning the simulation procedure and the potential parameters used.

Figure 1

The simulation box for the simulations presented here was cubic, with periodic boundary conditions in all three directions of space, and contained 150 DeTA⁺ cations, 150 bromide counterions (thus keeping the overall charge neutral) and 7500 water molecules. The starting configuration was generated by randomly dispersing the surfactants and counterions in an empty box. Water molecules were then inserted, starting from a pre-equilibrated box of pure water, and eliminating any molecules that overlapped with the surfactants or counterions. The energy was then minimized to eliminate any unphysical short-range contacts between adjacent atoms, and this was followed by a 25 ns MD run in the NpT ensemble. The last 13 ns of this run were considered for sampling purposes (see section 3). The average box length after equilibration was 6.6 nm, which yields an overall surfactant concentration of 0.867 M. Surfactant aggregates were identified and counted using an adaptation of the Hoshen-Kopelman cluster-counting algorithm [30], in which two surfactant molecules were considered to belong to the same aggregate if any two of their last four tail sites were separated by less than 0.64 nm [14]. An aggregate was

considered to be a micelle if it was composed of more than 5 surfactant molecules. Several properties were then calculated for each micelle, and averaged over the entire sampling region. These include radial distribution functions (RDFs) between different atoms, radial density profiles measured outwards from the micelle center of mass (COM), and molecular orientation distributions.

3. Results and Discussion

Immediately after the start of the simulation, surfactant molecules quickly assembled into small disordered aggregates of about 5-6 molecules. This very fast stage (about 50 ps) was then followed by a slower stage (~800 ps) in which smaller aggregates dissolved in favor of larger and more stable aggregates. At the end of this stage, analogous to the Ostwald ripening process commonly observed in colloidal systems [31], the solution was composed of a population of small micelles and isolated monomers. Micelle growth then proceeded even more slowly (~10 ns) by occasional fusion events, eventually reaching a plateau in the average cluster size. The entire mechanism and kinetics of the self-assembly process were described in detail in previous publications [6,14]. This paper is devoted to a more in-depth analysis of the structure of micelles, with properties being averaged over the plateau region (about 13 ns in total).

Figure 2a shows the micelle size distribution obtained by averaging over the sampling period, while a typical snapshot of a cross-section of the simulation box is shown in Figure 2b. A bimodal distribution was obtained, composed of a peak for isolated surfactant monomers and a well-defined peak for micelles, centered around 15 surfactants. Even though this system contains many more micelles than previous atomistic simulation studies, it is still too small to obtain a smooth size distribution. Nevertheless, the bimodal distribution presented in Figure 2 is in qualitative agreement with experimental expectations [1,2]. From the snapshot of Figure 2b, one can see that, despite the relatively high surfactant concentration, the micelles in the plateau region

are quite stable and far apart from each other. The mass-average micelle size for this system is 16, which is somewhat lower than experimental values for the same system (between 31 and 40 [32-36]) and simulations at a higher temperature [14], which implies that the present simulations at 298 K may not have reached full thermodynamic equilibrium (although the long duration of the plateau region, the high stability of individual micelles, and the bimodal shape of the micelle distribution suggest that they have at least reached a “pseudo-equilibrium” state). In fact, although the early stages of DeTAB self-assembly take place rather quickly, the later stages, when the system is close to equilibrium, proceed by very rare micelle fusion and breakage events, the frequency of which is significantly reduced at low temperature. Nevertheless, as will be discussed below, the structure of the small micelles obtained in the present simulations is very similar to previous simulations of larger micelles [7,9,14], and is thus likely to be representative of a fully equilibrated solution.

Figure 2

Figure 3 shows snapshots of two typical micelles obtained in the simulations, with surrounding water molecules removed. The micelles are roughly spherical, with a slight tendency for a prolate ellipsoid shape, in agreement with previous simulation results starting from a perfectly spherical pre-formed micelle [7]. The tail atoms organize themselves at the core of the micelle, while the head groups are located at the surface. A diffuse layer of bromide counterions completes the picture.

Figure 3

The micellar structure can be quantitatively characterized using radial density profiles, calculated by averaging the density of each atom type in spherical slabs of width 0.05 nm at increasing distances from the micelle COM. Such profiles are shown in Figure 4 for micelles composed of 15 or 16 surfactants (corresponding to the peak in the distribution of Figure 2). The hydrophobic micelle core is completely dry, with a density close to that of liquid nonane. An

analysis of the tail configurations yielded results that are very similar to a previous simulation study with the same surfactant [7]. Thus, the tail region of the DeTAB surfactant behaves similarly to a liquid alkane when organized in the core of a micelle. The density profile for the head groups has an approximately Gaussian shape, and marks a relatively sharp transition between hydrophobic and hydrophilic environments. The bromide layer is more diffuse, and the peak of the distribution is located approximately 0.35 nm away from the peak of the head-group layer. This suggests that most charge-neutralizing bromide ions are located rather close to the cationic surfactant heads. Interestingly, the water density profile begins to rise close to the beginning of the head-group layer, suggesting that water is able to penetrate into the micelle as far as the inner head site (EH in Figure 1).

Figure 4

More detailed information about the relative location of different molecules in the micelle can be gleaned by analyzing atomic radial distribution functions. These were computed in spherical slabs of width 0.005 nm at increasing distances from a given central atom. Figure 5 shows RDFs involving the nitrogen atom of the surfactant. The N-Br curve shows a pronounced maximum at 0.51 nm, evidencing close contact between bromide counterions and head groups. Using the Van der Waals diameters for the head methyl groups (0.35 nm) and the bromide ions (0.462 nm), together with the N-C bond length (0.147 nm), one can estimate the distance between the N atom and an adjacent Br. This rough estimate yields 0.55 nm, which is close to the location of the RDF peak, thus showing that Br ions associate with the head groups without intervening water molecules. The fraction of bound counterions for the simulated system, calculated from the number of Br ions within the first peak of the N-Br RDF, was 0.61. This is close to, but somewhat lower than, several experimental estimates [37-42].

Figure 5

The RDF between N and water oxygen atoms (Ow), shown as the thin line in Figure 5, exhibits a prominent peak at 0.46 nm, which once again is close to an estimate of 0.48 nm based on the respective Van der Waals diameters. This means that the first solvation shell of the head groups is composed of both water molecules and strongly bound bromide ions. This was corroborated by analysis of RDFs involving MH sites. Both the N-Br and the N-Ow curves show a small but well-defined second peak, which is the signature of a second solvation shell for the head groups. The main peak for the N-N RDF (dashed line in Figure 5) is located at about 0.85 nm, i.e. within the second solvation shell. The picture arising from the RDFs is consistent with conclusions based on the radial density profiles (Figure 4), and is in excellent agreement with a recent dielectric spectroscopic study of alkyltrimethylammonium bromide solutions [43].

Figure 6

Figure 6 shows RDFs involving water atoms and several different surfactant sites. From Figure 6a, one can immediately observe a close interaction between water oxygens and the outer head sites (MH). This is reflected in a broader peak for the interaction between water hydrogens (Hw) and MH sites (Figure 6b). The EH-Ow curve also shows a small peak at a similar distance than for MH-Ow, which means that water oxygens are bonded also to the inner head sites, but this peak vanishes for the RDFs between water and the tail sites. This confirms our previous observation that water penetrates into the micelle as far as the head-group layer. Another interesting conclusion is obtained by comparing the RDFs for each site in Figures 6a and 6b. For both the outer head sites and the tail sites, the water hydrogen peak is located at approximately the same distance as the oxygen peak. However, this is not the case for the EH curves – the EH-Hw peak is further away than the EH-Ow first peak. This suggests a specific orientation of the water molecule in the inner region of the head-group layer, which will be analyzed in detail next.

As demonstrated in previous studies of planar water/organic and water/vapor interfaces, the orientation of a given water molecule requires a bivariate angle distribution in order to be

uniquely specified. Such bivariate orientation distributions for water molecules hydrating each micelle were thus calculated, using a procedure proposed by Jedlovszky et al. [15]. The two chosen angles for these bivariate distributions were: (i) the angle between the interface normal and the water dipolar vector (θ); (ii) the angle between the molecular normal vector and the projection of the interface normal onto the plane perpendicular to the dipolar vector (φ). With the above choice of vectors, an isotropic orientation of water leads to a uniform distribution in φ and $\cos(\theta)$, where φ falls into the range between 0 and 90° [15]. In the original method, as applied to planar interfaces, the interface normal coincides with the Cartesian coordinate axis perpendicular to the interface. In a micellar system, with a curved interface, defining the interface normal vector is not as straightforward. Here, it was defined as the vector joining the micelle COM to the oxygen atom of the water molecule under consideration, pointing toward the micelle COM. The reader is referred to the previous publications for further details about the calculation procedure [15,16].

Figure 7

The bivariate orientation distributions for water surrounding micelles composed of 15 or 16 surfactants are presented in Figure 7. Each panel corresponds to a slice of width 0.25 nm at a different distance from the micelle COM. The distribution for the water molecules that are closest to the micellar core (Figure 7a) shows two distinct peaks. The highest peak corresponds to a configuration in which one of the hydrogen atoms is pointing toward the micelle core, while the smallest peak corresponds to water oriented with both the dipole vector and the H-H vector perpendicular to the surface normal. As we move away from the micelle center (Figure 7b), the latter orientation takes precedence, and the first peak disappears. Water molecules that show this perpendicular orientation are located close to the inner head group, which is consistent with the information obtained from the RDFs of Figure 6. Moving even further out (Figure 7c), a third preferred orientation appears – water molecules with one of the hydrogen atoms pointing to the

outside of the micelle core. It is very interesting to notice that this sequence of preferred orientations observed in the micelle hydration layer is remarkably similar to the one exhibited by the outermost layer of interfacial water molecules at planar interfaces [15-18]. This corroborates previous conclusions that the structure and orientation of the water phase is mostly independent of the nature of the opposite phase [17,18].

In the case of planar water/organic and water/vapor interfaces, water molecules beyond the first interfacial layer quickly recover the isotropic orientation of bulk [15-18]. In the micellar system, however, there is another distinct layer of water molecules whose dipole vector is oriented toward the micelle core (Figure 7d). This orientation corresponds to water molecules located between the head group layer and the bromide counterion layer (cf. Figure 4). Such molecules are expected to be highly polarized by the electrical double layer formed at the micelle surface, and thus orient themselves with their negatively charged oxygen atoms close to the cationic head groups and their positively charged hydrogens close to the bromide anions. Beyond this polarized layer, water molecules do indeed recover the bulk isotropic orientation (Figure 7f). It is worth noting that including polarizability in the molecular models tends to cause an increase in the interfacial activity of ions [44,45]. Thus, it would be interesting to know if polarizability will have a significant effect on the degree of counterion binding to the DeTAB micelles or on the orientation of water molecules in the highly polarized surface layer. However, such a study is outside the scope of this paper and is left for future work.

4. Conclusions

In this paper, a detailed study of the structure of cationic surfactant micelles in water, based on molecular simulations using an atomistic model, was presented. An important advantage relative to previous studies based on pre-formed aggregates is that the micelles were formed spontaneously from a direct simulation of the self-assembly process. Thus, no *a priori*

assumptions regarding the size, shape and structure of the aggregates were necessary. Furthermore, a novel method to determine the orientation of interfacial water molecules, previously applied only to planar systems, was applied here to the highly curved micelle/water interface, together with the calculation of radial distribution functions and density profiles. This analysis showed that the micelle core is dry and is composed of only tail atoms, forming an environment that is rather similar to a liquid alkane. The environment becomes hydrophilic as one moves past the well-defined layer of head-group atoms, with water molecules penetrating the micelle as far as the innermost head site. The first solvation layer of the micelle surface is composed of bromide ions, tightly bound to the cationic head groups, and water molecules that are highly polarized due to the electrical double layer at the exterior of the micelle. The water molecules that are located in the inner region of the head-group layer adopt a sequence of preferred orientations that is very similar to the one observed at planar interfaces with vapor or immiscible organic liquids. This strongly suggests that the structure of interfacial water molecules is practically unaffected by the nature and the curvature of the interface.

Acknowledgments:

The author acknowledges Mónica N. S. Oliveira for her help with the two-dimensional orientation plots and for fruitful discussions.

References:

- [1] Israelachvili, J. N. *Intermolecular and Surface Forces*, Academic Press: London, UK, 1985.
- [2] Gelbart, W. M.; Ben-Shaul, A. *J. Phys. Chem.* 100 (1996) 13169.
- [3] Shelley, J. C.; Shelley, M. Y. *Curr. Opin. Colloid Interface Sci* 5 (2000) 101.

- [4] Jorge, M.; Gomes, J. R. B.; Cordeiro, M. N. D. S.; Seaton, N. A. *J. Am. Chem. Soc.* 129 (2007) 15414.
- [5] Gomes, J. R. B.; Cordeiro, M. N. D. S.; Jorge, M. *Geochim. Cosmochim. Acta* 72 (2008) 4421.
- [6] Jorge, M.; Gomes, J. R. B.; Cordeiro, M. N. D. S.; Seaton, N. A. *J. Phys. Chem. B* 113 (2009) 708.
- [7] Böcker, J.; Brickmann, J.; Bopp, P. *J. Phys. Chem.* 98 (1994) 712.
- [8] Piotrovskaya, E. M.; Vanin, A. A.; Smirnova, N. A. *Mol. Phys.* 104 (2006) 3645.
- [9] Pal, S.; Bagchi, B.; Balasubramanian, S. *J. Phys. Chem.* 109 (2005) 12879.
- [10] Tarek, M.; Bandyopadhyay, S.; Klein, M. L. *J. Mol. Liq.* 78 (1998) 1.
- [11] Maillet, J.-B.; Lachet, V.; Coveney, P. V. *Phys. Chem. Chem. Phys.* 1 (1999) 5277.
- [12] Salaniwal, S.; Cui, S. T.; Cummings, P. T.; Cochran, H. D. *Langmuir* 15 (1999) 5188.
- [13] Marrink, S. J.; Tieleman, D. P.; Mark, A. E. *J. Phys. Chem. B* 104 (2000) 12165.
- [14] Jorge, M. *Langmuir* 24 (2008) 5714.
- [15] Jedlovsky, P.; Vincze, A.; Horvai, G. *J. Chem. Phys.* 117 (2002) 2271.
- [16] Jorge, M.; Cordeiro, M. N. D. S. *J. Phys. Chem. C* 111 (2007) 17612.
- [17] Jorge, M.; Cordeiro, M. N. D. S. *J. Phys. Chem. B* 112 (2008) 2415.
- [18] Pártay, L. B.; Hantal, G.; Jedlovsky, P.; Vincze, A.; Horvai, G. *J. Comput. Chem.* 29 (2008) 945.
- [19] Berendsen, H. J. C.; van der Spoel, D.; van Drunen, R. *Comput. Phys. Comm.* 91 (1995) 43.
- [20] Lindahl, E.; Hess, B.; van der Spoel, D. *J. Mol. Mod.* 7 (2001) 306.
- [21] Hockney, R. W.; Goel, S. P. J. *J. Comput. Phys.* 14 (1974) 148.
- [22] Nosé, S. *Mol. Phys.* 52 (1984) 255.
- [23] Hoover, W. G. *Phys. Rev. A* 31 (1985) 1695.

- [24] Parrinello, M.; Rahman, A. *J. Appl. Phys.* 52 (1981) 7182.
- [25] Hess, B.; Bekker, H.; Berendsen, H. J. C.; Fraaije, J. G. E. M. *J. Comp. Chem.* 18 (1997) 1463.
- [26] Essman, U.; Perela, L.; Berkowitz, M. L.; Darden, T.; Lee, H.; Pedersen, L. G. *J. Chem. Phys.* 103 (1995) 8577.
- [27] Berendsen, H. J. C.; Grigera, J. R.; Straatsma, T. P. *J. Phys. Chem.* 91 (1997) 6269.
- [28] Jorgensen, W. L.; Gao, J. *J. Phys. Chem.* 90 (1986) 2174.
- [29] Smit, B.; Karaborni, S.; Siepmann, J. I. *J. Chem. Phys.* 102 (1995) 2126.
- [30] Hoshen, J.; Kopelman, R. *Phys. Rev. B* 14 (1976) 3438.
- [31] Ratke, L.; Voorhees, P. W. (Eds) *Growth and Coarsening: Ostwald Ripening in Material Processing*; Springer-Verlag Telos: New York, 2002.
- [32] D'Errico, G.; Ortona, O.; Paduano, L.; Vitagliano, V. *J. Colloid Interface Sci.* 239 (2001) 264.
- [33] Yoshida, N.; Matsuoka, K.; Moroi, Y. *J. Colloid Interface Sci.* 187 (1997) 388.
- [34] Nomura, H.; Koda, S.; Matsuoka, T.; Hiyama, T.; Shibata, R.; Kato, S. *J. Colloid Interface Sci.* 230 (2000) 22.
- [35] Evans, D. F.; Allen, M.; Ninham, B. W.; Fouda, A. *J. Sol. Chem.* 13 (1984) 87.
- [36] Dorrance, R. C.; Hunter, T. F. *J. Chem. Soc., Faraday Trans. 1* 70 (1974) 1572.
- [37] Ribeiro, A. C. F.; Lobo, V. M. M.; Valente, A. J. M.; Azevedo, E. F. G.; Miguel M. G.; Burrows, H. D. *Colloid Polym. Sci.* 283 (2004) 277.
- [38] Evans, D. F.; Allen, M.; Ninham, B. W.; Fouda, A. *J. Sol. Chem.* 13 (1984) 87.
- [39] Zana, R. *J. Colloid Interface Sci.* 78 (1980) 330.
- [40] de Lisi, R.; Gradzielski, M.; Lazzara, G.; Milioto, S.; Muratore, N.; Prevost, S. *J. Phys. Chem. B* 110 (2006) 25883.

- [41] del Rio, J. M.; Pombo, C.; Prieto, G.; Mosquera, V.; Sarmiento, F. J. *Colloid Interface Sci.* 172 (1995) 137.
- [42] Mosquera, V.; del Rio, J. M.; Attwood, D.; Garcia, M.; Jones, M. N.; Prieto, G.; Suarez, M. J.; Sarmiento, F. J. *Colloid Interface Sci.* 206 (1998) 66.
- [43] Buchner, R.; Baar, C.; Fernandez, P.; Schrödle, S.; Kunz, W. *J. Mol. Liq.* 118 (2005) 179.
- [44] Jungwirth, P.; Tobias D. J. *J. Phys. Chem. B* 106 (2002) 6361.
- [45] Mucha, M.; Frigato, T.; Levering, L. M.; Allen, H. C.; Tobias, D. J.; Dang, L. X.; Jungwirth, P. *J. Phys. Chem. B* 109 (2005) 7617.

ACCEPTED MANUSCRIPT

Figure 1. Diagram of a DeTA⁺ cation with the nomenclature for site types: N corresponds to a nitrogen atom, MH is a methyl group belonging to the surfactant head, EH is a head methylene group, MT is a tail methyl group and ET is a tail methylene group.

Figure 2. a) Micelle size distribution averaged over the last 13 ns of simulation time; b) Snapshot of a cross-section of the simulation box obtained in the plateau region, showing three individual stable micelles. Surfactant tail atoms are represented by green spheres, head atoms by purple spheres, hydrogen atoms by white spheres, bromide ions by grey spheres, and oxygen atoms by blue spheres.

Figure 3. Snapshots of two typical micelles obtained during the simulation run. Color coding is the same as in Figure 2b, and water molecules have been omitted for clarity.

Figure 4. Radial density profiles, measured outward from the micelle center of mass, for micelles containing 15 or 16 surfactant molecules.

Figure 5. Radial distribution functions between surfactant nitrogen atoms and other atoms in the system: thin line – water oxygens; thick line – bromide ions; dashed line – nitrogen atoms.

Figure 6. Radial distribution functions between aliphatic sites in the surfactant molecule and water oxygens (a) and hydrogens (b): MH outer head sites (thin line); EH inner head sites (thick line); ET1 first tail site (thin dashed line); ET2 second tail site (thick dashed line).

Figure 7. Bivariate orientation distributions of water molecules hydrating DeTAB micelles with 15 or 16 surfactants, calculated in spherical slices perpendicular to the interface normal vector at different distances from the micelle COM: a) 0.5 to 0.75 nm; b) 0.75 to 1.0 nm; c) 1.0 to 1.25 nm; d) 1.25 to 1.5 nm; e) 1.5 to 1.75 nm; f) 1.75 to 2.0 nm. In the two-dimensional plots, red corresponds to high normalized probability and blue to low probability.

